

Study of the decay $D_s^+ \rightarrow K_S^0 K_S^0 \pi^+$ and observation an isovector partner to $f_0(1710)$

M. Ablikim¹, M. N. Achasov^{10,b}, P. Adlarson⁶⁸, S. Ahmed¹⁴, M. Albrecht⁴, R. Aliberti²⁸, A. Amoroso^{67A,67C}, M. R. An³², Q. An^{64,50}, X. H. Bai⁵⁸, Y. Bai⁴⁹, O. Bakina²⁹, R. Baldini Ferroli^{23A}, I. Balossino^{24A}, Y. Ban^{39,h}, K. Begzsuren²⁶, N. Berger²⁸, M. Bertani^{23A}, D. Bettoni^{24A}, F. Bianchi^{67A,67C}, J. Bloms⁶¹, A. Bortone^{67A,67C}, I. Boyko²⁹, R. A. Briere⁵, H. Cai⁶⁹, X. Cai^{1,50}, A. Calcaterra^{23A}, G. F. Cao^{1,55}, N. Cao^{1,55}, S. A. Cetin^{54A}, J. F. Chang^{1,50}, W. L. Chang^{1,55}, G. Chelkov^{29,a}, D. Y. Chen⁶, G. Chen¹, H. S. Chen^{1,55}, M. L. Chen^{1,50}, S. J. Chen³⁵, X. R. Chen²⁵, Y. B. Chen^{1,50}, Z. J. Chen^{20,i}, W. S. Cheng^{67C}, G. Cibinetto^{24A}, F. Cossio^{67C}, X. F. Cui³⁶, H. L. Dai^{1,50}, X. C. Dai^{1,55}, A. Dbeysssi¹⁴, R. E. de Boer⁴, D. Dedovich²⁹, Z. Y. Deng¹, A. Denig²⁸, I. Denysenko²⁹, M. Destefanis^{67A,67C}, F. De Mori^{67A,67C}, Y. Ding³³, C. Dong³⁶, J. Dong^{1,50}, L. Y. Dong^{1,55}, M. Y. Dong^{1,50,55}, X. Dong⁶⁹, S. X. Du⁷², Y. L. Fan⁶⁹, J. Fang^{1,50}, S. S. Fang^{1,55}, Y. Fang¹, R. Farinelli^{24A}, L. Fava^{67B,67C}, F. Feldbauer⁴, G. Felici^{23A}, C. Q. Feng^{64,50}, J. H. Feng⁵¹, M. Fritsch⁴, C. D. Fu¹, Y. Gao^{64,50}, Y. Gao^{39,h}, Y. G. Gao⁶, I. Garzia^{24A,24B}, P. T. Ge⁶⁹, C. Geng⁵¹, E. M. Gersabeck⁵⁹, A. Gilman⁶², K. Goetzen¹¹, L. Gong³³, W. X. Gong^{1,50}, W. Gradl²⁸, M. Greco^{67A,67C}, L. M. Gu³⁵, M. H. Gu^{1,50}, C. Y. Guan^{1,55}, A. Q. Guo²⁵, A. Q. Guo²², L. B. Guo³⁴, R. P. Guo⁴¹, Y. P. Guo^{9,f}, A. Guskov^{29,a}, T. T. Han⁴², W. Y. Han³², X. Q. Hao¹⁵, F. A. Harris⁵⁷, K. L. He^{1,55}, F. H. Heinsius⁴, C. H. Heinz²⁸, Y. K. Heng^{1,50,55}, C. Herold⁵², M. Himmelreich^{11,d}, T. Holtmann⁴, G. Y. Hou^{1,55}, Y. R. Hou⁵⁵, Z. L. Hou¹, H. M. Hu^{1,55}, J. F. Hu^{48,j}, T. Hu^{1,50,55}, Y. Hu¹, G. S. Huang^{64,50}, L. Q. Huang⁶⁵, X. T. Huang⁴², Y. P. Huang¹, Z. Huang^{39,h}, T. Hussain⁶⁶, N. Hüsken^{22,28}, W. Ikegami Andersson⁶⁸, W. Imoehl²², M. Irshad^{64,50}, S. Jaeger⁴, S. Janchiv²⁶, Q. Ji¹, Q. P. Ji¹⁵, X. B. Ji^{1,55}, X. L. Ji^{1,50}, Y. Y. Ji⁴², H. B. Jiang⁴², X. S. Jiang^{1,50,55}, J. B. Jiao⁴², Z. Jiao¹⁸, S. Jin³⁵, Y. Jin⁵⁸, M. Q. Jing^{1,55}, T. Johansson⁶⁸, N. Kalantar-Nayestanaki⁵⁶, X. S. Kang³³, R. Kappert⁵⁶, M. Kavatsyuk⁵⁶, B. C. Ke⁷², I. K. Keshk⁴, A. Khoukaz⁶¹, P. Kiese²⁸, R. Kiuchi¹, R. Kliemt¹¹, L. Koch³⁰, O. B. Kolcu^{54A,m}, B. Kopf⁴, M. Kuemmel⁴, M. Kuessner⁴, A. Kupsc^{37,68}, M. G. Kurth^{1,55}, W. Kühn³⁰, J. J. Lane⁵⁹, J. S. Lange³⁰, P. Larin¹⁴, A. Lavania²¹, L. Lavezzi^{67A,67C}, Z. H. Lei^{64,50}, H. Leithoff²⁸, M. Lellmann²⁸, T. Lenz²⁸, C. Li⁴⁰, C. H. Li³², Cheng Li^{64,50}, D. M. Li⁷², F. Li^{1,50}, G. Li¹, H. Li^{64,50}, H. Li⁴⁴, H. B. Li^{1,55}, H. J. Li¹⁵, H. N. Li^{48,j}, J. L. Li⁴², J. Q. Li⁴, J. S. Li⁵¹, Ke Li¹, L. K. Li¹, Lei Li³, P. R. Li^{31,k,l}, S. Y. Li⁵³, W. D. Li^{1,55}, W. G. Li¹, X. H. Li^{64,50}, X. L. Li⁴², Xiaoyu Li^{1,55}, Z. Y. Li⁵¹, H. Liang^{64,50}, H. Liang^{1,55}, H. Liang²⁷, Y. F. Liang⁴⁶, Y. T. Liang²⁵, G. R. Liao¹², L. Z. Liao^{1,55}, J. Libby²¹, C. X. Lin⁵¹, D. X. Lin²⁵, T. Lin¹, B. J. Liu¹, C. X. Liu¹, D. Liu^{14,64}, F. H. Liu⁴⁵, Fang Liu¹, Feng Liu⁶, G. M. Liu^{48,j}, H. M. Liu^{1,55}, Huanhuan Liu¹, Huihui Liu¹⁶, J. B. Liu^{64,50}, J. L. Liu⁶⁵, J. Y. Liu^{1,55}, K. Liu¹, K. Y. Liu³³, Ke Liu¹⁷, L. Liu^{64,50}, M. H. Liu^{9,f}, P. L. Liu¹, Q. Liu⁵⁵, Q. Liu⁶⁹, S. B. Liu^{64,50}, T. Liu^{1,55}, W. M. Liu^{64,50}, X. Liu^{31,k,l}, Y. Liu³⁶, Z. A. Liu^{1,50,55}, Z. Q. Liu⁴², X. C. Lou^{1,50,55}, F. X. Lu⁵¹, H. J. Lu¹⁸, J. D. Lu^{1,55}, J. G. Lu^{1,50}, X. L. Lu¹, Y. Lu¹, Y. P. Lu^{1,50}, C. L. Luo³⁴, M. X. Luo⁷¹, P. W. Luo⁵¹, T. Luo^{9,f}, X. L. Luo^{1,50}, X. R. Lyu⁵⁵, F. C. Ma³³, H. L. Ma¹, L. L. Ma⁴², M. M. Ma^{1,55}, Q. M. Ma¹, R. Q. Ma^{1,55}, R. T. Ma⁵⁵, X. X. Ma^{1,55}, X. Y. Ma^{1,50}, F. E. Maas¹⁴, M. Maggiora^{67A,67C}, S. Maldaner⁴, S. Malde⁶², Q. A. Malik⁶⁶, A. Mangoni^{23B}, Y. J. Mao^{39,h}, Z. P. Mao¹, S. Marcello^{67A,67C}, Z. X. Meng⁵⁸, J. G. Messchendorp⁵⁶, G. Mezzadri^{24A}, T. J. Min³⁵, R. E. Mitchell²², X. H. Mo^{1,50,55}, N. Yu. Muchnoi^{10,b}, H. Muramatsu⁶⁰, S. Nakhoul^{11,d}, Y. Nefedov²⁹, F. Nerling^{11,d}, I. B. Nikolaev^{10,b}, Z. Ning^{1,50}, S. Nisar^{8,g}, Q. Ouyang^{1,50,55}, S. Pacetti^{23B,23C}, X. Pan^{9,f}, Y. Pan⁵⁹, A. Pathak¹, A. Pathak²⁷, P. Patteri^{23A}, M. Pelizzaeus⁴, H. P. Peng^{64,50}, K. Peters^{11,d}, J. Pettersson⁶⁸, J. L. Ping³⁴, R. G. Ping^{1,55}, S. Pogodin²⁹, R. Poling⁶⁰, V. Prasad^{64,50}, H. Qi^{64,50}, H. R. Qi⁵³, M. Qi³⁵, T. Y. Qi⁹, S. Qian^{1,50}, W. B. Qian⁵⁵, Z. Qian⁵¹, C. F. Qiao⁵⁵, J. J. Qin⁶⁵, L. Q. Qin¹², X. P. Qin⁹, X. S. Qin⁴², Z. H. Qin^{1,50}, J. F. Qiu¹, S. Q. Qu³⁶, K. H. Rashid⁶⁶, K. Ravindran²¹, C. F. Redmer²⁸, A. Rivetti^{67C}, V. Roinin⁵⁶, M. Rolo^{67C}, G. Rong^{1,55}, Ch. Rosner¹⁴, M. Rump⁶¹, H. S. Sang⁶⁴, A. Sarantsev^{29,c}, Y. Schelhaas²⁸, C. Schnier⁴, K. Schoenning⁶⁸, M. Scodeggio^{24A,24B}, W. Shan¹⁹, X. Y. Shan^{64,50}, J. F. Shanguan⁴⁷, M. Shao^{64,50}, C. P. Shen⁹, H. F. Shen^{1,55}, X. Y. Shen^{1,55}, H. C. Shi^{64,50}, R. S. Shi^{1,55}, X. Shi^{1,50}, X. D. Shi^{64,50}, J. J. Song¹⁵, J. J. Song⁴², W. M. Song^{27,1}, Y. X. Song^{39,h}, S. Sosio^{67A,67C}, S. Spataro^{67A,67C}, K. X. Su⁶⁹, P. P. Su⁴⁷, F. F. Sui⁴², G. X. Sun¹, H. K. Sun¹, J. F. Sun¹⁵, L. Sun⁶⁹, S. S. Sun^{1,55}, T. Sun^{1,55}, W. Y. Sun²⁷, X. Sun^{20,i}, Y. J. Sun^{64,50}, Y. Z. Sun¹, Z. T. Sun¹, Y. H. Tan⁶⁹, Y. X. Tan^{64,50}, C. J. Tang⁴⁶, G. Y. Tang¹, J. Tang⁵¹, J. X. Teng^{64,50}, V. Thoren⁶⁸, W. H. Tian⁴⁴, Y. T. Tian²⁵, I. Uman^{54B}, B. Wang¹, C. W. Wang³⁵, D. Y. Wang^{39,h}, H. J. Wang^{31,k,l}, H. P. Wang^{1,55}, K. Wang^{1,50}, L. L. Wang¹, M. Wang⁴², M. Z. Wang^{39,h}, Meng Wang^{1,55}, S. Wang^{9,f}, W. Wang⁵¹, W. H. Wang⁶⁹, W. P. Wang^{64,50}, X. Wang^{39,h}, X. F. Wang^{31,k,l}, X. L. Wang^{9,f}, Y. Wang⁵¹, Y. D. Wang³⁸, Y. F. Wang^{1,50,55}, Y. Q. Wang¹, Y. Y. Wang^{31,k,l}, Z. Wang^{1,50}, Z. Y. Wang¹, Ziyi Wang⁵⁵, Zongyuan Wang^{1,55}, D. H. Wei¹², F. Weidner⁶¹, S. P. Wen¹, D. J. White⁵⁹, U. Wiedner⁴, G. Wilkinson⁶², M. Wolke⁶⁸, L. Wollenberg⁴, J. F. Wu^{1,55}, L. H. Wu¹, L. J. Wu^{1,55}, X. Wu^{9,f}, X. H. Wu²⁷, Z. Wu^{1,50}, L. Xia^{64,50}, H. Xiao^{9,f}, S. Y. Xiao¹, Z. J. Xiao³⁴, X. H. Xie^{39,h}, Y. G. Xie^{1,50}, Y. H. Xie⁶, T. Y. Xing^{1,55}, C. J. Xu⁵¹, G. F. Xu¹, Q. J. Xu¹³, W. Xu^{1,55}, X. P. Xu⁴⁷, Y. C. Xu⁵⁵, F. Yan^{9,f}, L. Yan^{9,f}, W. B. Yan^{64,50}, W. C. Yan⁷², H. J. Yang^{43,e}, H. X. Yang¹, L. Yang⁴⁴, S. L. Yang⁵⁵, Y. X. Yang¹², Yifan Yang^{1,55}, Zhi Yang²⁵, M. Ye^{1,50}, M. H. Ye⁷, J. H. Yin¹, Z. Y. You⁵¹, B. X. Yu^{1,50,55}, C. X. Yu³⁶, G. Yu^{1,55}, J. S. Yu^{20,i}, T. Yu⁶⁵, C. Z. Yuan^{1,55}, L. Yuan², X. Q. Yuan^{39,h}, Y. Yuan¹, Z. Y. Yuan⁵¹, C. X. Yue³², A. A. Zafar⁶⁶, X. Zeng Zeng⁶, Y. Zeng^{20,i}, A. Q. Zhang¹, B. X. Zhang¹, Guangyi Zhang¹⁵, H. Zhang⁶⁴, H. H. Zhang⁵¹, H. H. Zhang²⁷, H. Y. Zhang^{1,50}, J. J. Zhang⁴⁴, J. L. Zhang⁷⁰, J. Q. Zhang³⁴, J. W. Zhang^{1,50,55}, J. Y. Zhang¹, J. Z. Zhang^{1,55}, Jianyu Zhang^{1,55}, Jiawei Zhang^{1,55}, L. M. Zhang⁵³, L. Q. Zhang⁵¹, Lei Zhang³⁵, S. Zhang⁵¹, S. F. Zhang³⁵, Shulei Zhang^{20,i}, X. D. Zhang³⁸, X. Y. Zhang⁴², Y. Zhang⁶², Y. T. Zhang⁷², Y. H. Zhang^{1,50}, Yan Zhang^{64,50}, Yao Zhang¹, Z. Y. Zhang⁶⁹, G. Zhao¹, J. Zhao³², J. Y. Zhao^{1,55}, J. Z. Zhao^{1,50}, Lei Zhao^{64,50}, Ling Zhao¹, M. G. Zhao³⁶, Q. Zhao¹, S. J. Zhao⁷², Y. B. Zhao^{1,50}, Y. X. Zhao²⁵, Z. G. Zhao^{64,50}, A. Zhemchugov^{29,a}, B. Zheng⁶⁵, J. P. Zheng^{1,50}, Y. H. Zheng⁵⁵, B. Zhong³⁴, C. Zhong⁶⁵, L. P. Zhou^{1,55}, Q. Zhou^{1,55}, X. Zhou⁶⁹, X. K. Zhou⁵⁵, X. R. Zhou^{64,50}, X. Y. Zhou³², A. N. Zhu^{1,55}, J. Zhu³⁶, K. Zhu¹, K. J. Zhu^{1,50,55}, S. H. Zhu⁶³, T. J. Zhu⁷⁰, W. J. Zhu³⁶, W. J. Zhu^{9,f}, Y. C. Zhu^{64,50}, Z. A. Zhu^{1,55}, B. S. Zou¹, J. H. Zou¹

(BESIII Collaboration)

- ¹ Institute of High Energy Physics, Beijing 100049, People's Republic of China
- ² Beihang University, Beijing 100191, People's Republic of China
- ³ Beijing Institute of Petrochemical Technology, Beijing 102617, People's Republic of China
- ⁴ Bochum Ruhr-University, D-44780 Bochum, Germany
- ⁵ Carnegie Mellon University, Pittsburgh, Pennsylvania 15213, USA
- ⁶ Central China Normal University, Wuhan 430079, People's Republic of China
- ⁷ China Center of Advanced Science and Technology, Beijing 100190, People's Republic of China
- ⁸ COMSATS University Islamabad, Lahore Campus, Defence Road, Off Raiwind Road, 54000 Lahore, Pakistan
- ⁹ Fudan University, Shanghai 200443, People's Republic of China
- ¹⁰ G.I. Budker Institute of Nuclear Physics SB RAS (BINP), Novosibirsk 630090, Russia
- ¹¹ GSI Helmholtzcentre for Heavy Ion Research GmbH, D-64291 Darmstadt, Germany
- ¹² Guangxi Normal University, Guilin 541004, People's Republic of China
- ¹³ Hangzhou Normal University, Hangzhou 310036, People's Republic of China
- ¹⁴ Helmholtz Institute Mainz, Staudinger Weg 18, D-55099 Mainz, Germany
- ¹⁵ Henan Normal University, Xinxiang 453007, People's Republic of China
- ¹⁶ Henan University of Science and Technology, Luoyang 471003, People's Republic of China
- ¹⁷ Henan University of Technology, Zhengzhou 450001, People's Republic of China
- ¹⁸ Huangshan College, Huangshan 245000, People's Republic of China
- ¹⁹ Hunan Normal University, Changsha 410081, People's Republic of China
- ²⁰ Hunan University, Changsha 410082, People's Republic of China
- ²¹ Indian Institute of Technology Madras, Chennai 600036, India
- ²² Indiana University, Bloomington, Indiana 47405, USA
- ²³ INFN Laboratori Nazionali di Frascati, (A)INFN Laboratori Nazionali di Frascati, I-00044, Frascati, Italy; (B)INFN Sezione di Perugia, I-06100, Perugia, Italy; (C)University of Perugia, I-06100, Perugia, Italy
- ²⁴ INFN Sezione di Ferrara, (A)INFN Sezione di Ferrara, I-44122, Ferrara, Italy; (B)University of Ferrara, I-44122, Ferrara, Italy
- ²⁵ Institute of Modern Physics, Lanzhou 730000, People's Republic of China
- ²⁶ Institute of Physics and Technology, Peace Ave. 54B, Ulaanbaatar 13330, Mongolia
- ²⁷ Jilin University, Changchun 130012, People's Republic of China
- ²⁸ Johannes Gutenberg University of Mainz, Johann-Joachim-Becher-Weg 45, D-55099 Mainz, Germany
- ²⁹ Joint Institute for Nuclear Research, 141980 Dubna, Moscow region, Russia
- ³⁰ Justus-Liebig-Universität Giessen, II. Physikalisches Institut, Heinrich-Buff-Ring 16, D-35392 Giessen, Germany
- ³¹ Lanzhou University, Lanzhou 730000, People's Republic of China
- ³² Liaoning Normal University, Dalian 116029, People's Republic of China
- ³³ Liaoning University, Shenyang 110036, People's Republic of China
- ³⁴ Nanjing Normal University, Nanjing 210023, People's Republic of China
- ³⁵ Nanjing University, Nanjing 210093, People's Republic of China
- ³⁶ Nankai University, Tianjin 300071, People's Republic of China
- ³⁷ National Centre for Nuclear Research, Warsaw 02-093, Poland
- ³⁸ North China Electric Power University, Beijing 102206, People's Republic of China
- ³⁹ Peking University, Beijing 100871, People's Republic of China
- ⁴⁰ Qufu Normal University, Qufu 273165, People's Republic of China
- ⁴¹ Shandong Normal University, Jinan 250014, People's Republic of China
- ⁴² Shandong University, Jinan 250100, People's Republic of China
- ⁴³ Shanghai Jiao Tong University, Shanghai 200240, People's Republic of China
- ⁴⁴ Shanxi Normal University, Linfen 041004, People's Republic of China
- ⁴⁵ Shanxi University, Taiyuan 030006, People's Republic of China
- ⁴⁶ Sichuan University, Chengdu 610064, People's Republic of China
- ⁴⁷ Soochow University, Suzhou 215006, People's Republic of China
- ⁴⁸ South China Normal University, Guangzhou 510006, People's Republic of China
- ⁴⁹ Southeast University, Nanjing 211100, People's Republic of China
- ⁵⁰ State Key Laboratory of Particle Detection and Electronics, Beijing 100049, Hefei 230026, People's Republic of China
- ⁵¹ Sun Yat-Sen University, Guangzhou 510275, People's Republic of China
- ⁵² Suranaree University of Technology, University Avenue 111, Nakhon Ratchasima 30000, Thailand
- ⁵³ Tsinghua University, Beijing 100084, People's Republic of China
- ⁵⁴ Turkish Accelerator Center Particle Factory Group, (A)Istanbul Bilgi University, HEP Res. Cent., 34060 Eyup, Istanbul, Turkey; (B)Near East University, Nicosia, North Cyprus, Mersin 10, Turkey
- ⁵⁵ University of Chinese Academy of Sciences, Beijing 100049, People's Republic of China
- ⁵⁶ University of Groningen, NL-9747 AA Groningen, The Netherlands
- ⁵⁷ University of Hawaii, Honolulu, Hawaii 96822, USA
- ⁵⁸ University of Jinan, Jinan 250022, People's Republic of China
- ⁵⁹ University of Manchester, Oxford Road, Manchester, M13 9PL, United Kingdom

⁶⁰ University of Minnesota, Minneapolis, Minnesota 55455, USA

⁶¹ University of Muenster, Wilhelm-Klemm-Str. 9, 48149 Muenster, Germany

⁶² University of Oxford, Keble Rd, Oxford, UK OX13RH

⁶³ University of Science and Technology Liaoning, Anshan 114051, People's Republic of China

⁶⁴ University of Science and Technology of China, Hefei 230026, People's Republic of China

⁶⁵ University of South China, Hengyang 421001, People's Republic of China

⁶⁶ University of the Punjab, Lahore-54590, Pakistan

⁶⁷ University of Turin and INFN, (A)University of Turin, I-10125, Turin, Italy; (B)University of Eastern Piedmont, I-15121, Alessandria, Italy; (C)INFN, I-10125, Turin, Italy

⁶⁸ Uppsala University, Box 516, SE-75120 Uppsala, Sweden

⁶⁹ Wuhan University, Wuhan 430072, People's Republic of China

⁷⁰ Xinyang Normal University, Xinyang 464000, People's Republic of China

⁷¹ Zhejiang University, Hangzhou 310027, People's Republic of China

⁷² Zhengzhou University, Zhengzhou 450001, People's Republic of China

^a Also at the Moscow Institute of Physics and Technology, Moscow 141700, Russia

^b Also at the Novosibirsk State University, Novosibirsk, 630090, Russia

^c Also at the NRC "Kurchatov Institute", PNPI, 188300, Gatchina, Russia

^d Also at Goethe University Frankfurt, 60323 Frankfurt am Main, Germany

^e Also at Key Laboratory for Particle Physics, Astrophysics and Cosmology, Ministry of Education; Shanghai Key Laboratory for Particle Physics and Cosmology; Institute of Nuclear and Particle Physics, Shanghai 200240, People's Republic of China

^f Also at Key Laboratory of Nuclear Physics and Ion-beam Application (MOE) and Institute of Modern Physics, Fudan University, Shanghai 200443, People's Republic of China

^g Also at Harvard University, Department of Physics, Cambridge, MA, 02138, USA

^h Also at State Key Laboratory of Nuclear Physics and Technology, Peking University, Beijing 100871, People's Republic of China

ⁱ Also at School of Physics and Electronics, Hunan University, Changsha 410082, China

^j Also at Guangdong Provincial Key Laboratory of Nuclear Science, Institute of Quantum Matter, South China Normal University, Guangzhou 510006, China

^k Also at Frontiers Science Center for Rare Isotopes, Lanzhou University, Lanzhou 730000, People's Republic of China

^l Also at Lanzhou Center for Theoretical Physics, Lanzhou University, Lanzhou 730000, People's Republic of China

^m Currently at Istinye University, 34010 Istanbul, Turkey

(Dated: October 18, 2021)

Using e^+e^- annihilation data corresponding to a total integrated luminosity of 6.32 fb^{-1} collected at center-of-mass energies between 4.178 and 4.226 GeV with the BESIII detector, we perform an amplitude analysis of the decay $D_s^+ \rightarrow K_S^0 K_S^0 \pi^+$ for the first time. An enhancement is observed in the $K_S^0 K_S^0$ mass spectrum near $1.7 \text{ GeV}/c^2$, which was not seen in $D_s^+ \rightarrow K^+ K^- \pi^+$ in an earlier work, implying the existence of an isospin one partner of the $f_0(1710)$. The branching fraction of the decay $D_s^+ \rightarrow K_S^0 K_S^0 \pi^+$ is determined to be $\mathcal{B}(D_s^+ \rightarrow K_S^0 K_S^0 \pi^+) = (0.68 \pm 0.04_{\text{stat}} \pm 0.01_{\text{sys}})\%$.

The constituent quark model has been successful in explaining the composition of hadrons in the past few decades. In this model, many of the observed light mesons can be described as $q\bar{q}$ states grouped into SU(3) flavor multiplets. In a recent work [1, 2], the $f_0(500)$ and $f_0(980)$ mesons are considered to be the ground state SU(3) singlet and octet scalar isoscalar mesons, and the $a_0(980)$ meson is their isovector partner. The SU(3) singlet $f_0(1370)$ and octet $f_0(1500)$ are then considered to be the radial excited states of the $f_0(500)$ and $f_0(980)$ mesons, respectively, with an isovector partner in the $a_0(1450)$. However, in case of the next radial excitation in [1, 2], for the singlet $f_0(1710)$ and the newly-identified octet state $f_0(1770)$, no corresponding isovector $a_0(1710)$ meson has been established yet. The BaBar collaboration recently claimed the observation of a new $a_0(1710)^\pm$ resonance in the decay to $\pi^\pm \eta$ with a mass of approximately $1.7 \text{ GeV}/c^2$ in the $\eta_c \rightarrow \eta \pi^+ \pi^-$

decay [5]. Constructing isospin eigenstates from kaon pairs, we obtain $(|K^+ K^- \rangle - |K^0 \bar{K}^0 \rangle)$ for isospin one, but $(|K^+ K^- \rangle + |K^0 \bar{K}^0 \rangle)$ for isospin zero. It follows that if the interference between an f_0 and an a_0 is constructive in decays to a $K^+ K^-$ pair, it is destructive in decays to a pair of neutral kaons and vice versa. A comparison between decays involving $K^+ K^-$ and $K_S^0 K_S^0$ pairs can thus give access to such interference terms and allows a search for the $a_0(1710)^0$ in decays to two kaons.

The BESIII and the BaBar collaborations reported analyses of the $D_s^+ \rightarrow K^+ K^- \pi^+$ decay [3, 4] and observed contributions of the scalar mesons $S(980)$ (where $S(980)$ denotes an admixture of $a_0(980)^0$ and $f_0(980)$) and $f_0(1710)$. Both collaborations reported consistent results for the branching fractions (BF) $\mathcal{B}(D_s^+ \rightarrow S(980)\pi^+, S(980) \rightarrow K^+ K^-) = (1.05 \pm 0.04_{\text{stat}} \pm 0.06_{\text{sys}})\%$ and $\mathcal{B}(D_s^+ \rightarrow f_0(1710)\pi^+, f_0(1710) \rightarrow K^+ K^-) = (0.10 \pm 0.02_{\text{stat}} \pm 0.03_{\text{sys}})\%$ [3].

Furthermore, analyses of D_s decays are an important input for studies of the B_s^0 meson, which predominantly decays to $D_s + X$ [6]. In addition, hadronic D_s decays probe the interplay of short-distance weak-decay matrix elements and long-distance QCD interactions. The measurement of BFs of hadronic D_s decays provides valuable information to help understand strong force-induced amplitudes and phases [7–10].

The CLEO collaboration measured the absolute BF of the decay $D_s^+ \rightarrow K_S^0 K_S^0 \pi^+$ to be $(0.77 \pm 0.05_{\text{stat}} \pm 0.03_{\text{sys}})\%$ [11], using a dataset corresponding to a luminosity of 586 pb^{-1} at a center-of-mass energy of 4.17 GeV. In this work, we present the first amplitude analysis and a more precise measurement of the BF of the $D_s^+ \rightarrow K_S^0 K_S^0 \pi^+$ decay using 6.32 fb^{-1} of data samples collected at center-of-mass energies of 4.178, 4.189, 4.199, 4.209, 4.219 and 4.226 GeV with the BESIII detector. We do not distinguish between the $a_0(1710)^0$ and $f_0(1710)$ mesons, and denote the combined state as $S(1710)$. Charge conjugation is implied throughout this paper.

The BESIII detector [12, 13] records symmetric e^+e^- collisions provided by the BEPCII storage ring [14]. The cylindrical core of the BESIII detector covers 93% of the full solid angle and consists of a helium-based multilayer drift chamber (MDC), a plastic scintillator time-of-flight system (TOF), and a CsI(Tl) electromagnetic calorimeter (EMC), which are all enclosed in a superconducting solenoidal magnet providing a 1.0 T magnetic field. The end cap TOF system was upgraded in 2015 using multi-gap resistive plate chamber technology [15].

Simulated data samples produced with GEANT4-based [16] Monte Carlo (MC) software, which includes the geometric description of the BESIII detector and the detector response, are used to determine detection efficiencies and to estimate backgrounds. The simulation models the beam energy spread and initial state radiation (ISR) in the e^+e^- annihilations with the generator KKMC [17]. The inclusive MC sample includes the production of open charm processes, the ISR production of vector charmonium(-like) states, and the continuum processes incorporated in KKMC [17]. The known decay modes are modeled with EVTGEN [18] using BFs taken from the Particle Data Group [6], and the remaining unknown charmonium decays are modeled with LUNDCHARM [19]. Final state radiation (FSR) from charged final state particles is incorporated using PHOTOS [20].

The process $e^+e^- \rightarrow D_s^{*\pm} D_s^\mp \rightarrow \gamma D_s^+ D_s^-$ allows studies of D_s^+ decays with a tag technique [21]. There are two types of samples used in the tag technique: single tag (ST) and double tag (DT). In the ST sample, a D_s^- meson is reconstructed through a particular hadronic decay without any requirement on the remaining measured tracks and EMC showers. In the DT sample, a

D_s^+ , designated as the “signal”, is reconstructed through $D_s^+ \rightarrow K_S^0 K_S^0 \pi^+$, while a D_s^- , designated as “tag”, is reconstructed through one of eight hadronic decay modes: $D_s^- \rightarrow K_S^0 K^-$, $K^+ K^- \pi^-$, $K^+ K^- \pi^- \pi^0$, $K_S^0 K^- \pi^- \pi^+$, $K_S^0 K^+ \pi^- \pi^-$, $\pi^- \pi^- \pi^+$, $\pi^- \eta'$, and $K^- \pi^- \pi^+$. A detailed description of selection conditions concerning charged and neutral particle candidates, the mass recoiling against D_s^\pm candidates, and the mass of the tag candidates are provided in Refs. [22–24].

As in Refs. [23, 24], an eight-constraint (8C) kinematic fit is performed to select signal events for the amplitude analysis. Besides the constraints arising from four-momentum conservation, the invariant masses of the two K_S^0 candidates, the tag D_s^- , and the $D_s^{*+(-)}$ candidates are constrained to their known masses given in Ref. [6]. If there are multiple signal combinations, the candidate with the minimum χ^2 of the 8C kinematic fit is chosen. Signal D_s^+ candidates are selected if their invariant mass is in the interval $[1.950, 1.990] \text{ GeV}/c^2$. A further kinematic fit including a ninth constraint on the mass of the signal D_s^+ is performed, and the updated four-momenta are used for the amplitude analysis. This ensures that all candidates fall within the phase space boundary. In total, 412 events are selected with a purity of $f_s = (97.3 \pm 0.8)\%$. The purity is determined from a fit to the invariant mass distribution of the signal D_s^+ candidates.

This analysis uses an isobar formulation in the covariant tensor formalism [25]. The total amplitude M for the decay is described by a coherent sum of the amplitudes of all intermediate processes, $M = \sum_n c_n A_n$, where n indicates the n^{th} intermediate state and $c_n = \rho_n e^{i\phi_n}$ is the corresponding complex coefficient with magnitude ρ_n and phase ϕ_n . The model is symmetrized with respect to the two identical K_S^0 mesons. The two-body decay amplitude A_n is given by $A_n = P_n S_n F_n^r F_n^D$, where S_n and $F_n^{r(D)}$ are the spin factor [25] and the Blatt-Weisskopf barrier factor of the intermediate state (the D_s^\pm meson) [26], respectively, and P_n is the relativistic Breit-Wigner amplitude [27] describing the propagator of the intermediate resonance.

Contributions of intermediate resonances are determined by an unbinned maximum-likelihood fit to data. A combined probability density function (PDF) for the signal and background hypotheses is constructed, depending on the momenta of the three final-state particles. See Refs. [23, 24, 28] for details. The signal PDF is constructed from the total amplitude M . The background PDF, B , is constructed from a background shape derived from the inclusive MC samples using the kernel estimation method RooNDKeysPdf [29, 30]. It models the distribution of an input dataset as a superposition of Gaussian kernels. This background PDF is then added to the signal PDF incoherently and the combined PDF

is written as

$$\text{PDF} = \epsilon R_3 \left[\frac{f_s |M(p_j)|^2}{\int \epsilon |M(p_j)|^2 R_3 dp_j} + \frac{(1 - f_s) B_\epsilon(p_j)}{\int \epsilon B_\epsilon(p_j) R_3 dp_j} \right],$$

where B_ϵ is defined as B/ϵ , ϵ is the acceptance in bins of the Dalitz plot determined with a MC sample of $D_s^+ \rightarrow K_S^0 K_S^0 \pi^+$ uniformly distributed over the Dalitz plot. The placeholder $p_j = \{p_1, p_2, p_3\}$ represents the momenta of the final state particles, R_3 is the three-body phase-space element, and f_s is the purity. The normalization integral in the denominator is determined by a MC technique as described in Ref. [23, 24].

The Dalitz plot of $M_{K_S^0 \pi^+}^2$ versus $M_{K_S^0 K_S^0}^2$ is shown in Fig. 1(a). The strong vertical and horizontal bands around $0.8 \text{ GeV}^2/c^4$ are caused by the process $D_s^+ \rightarrow K_S^0 K^*(892)^+$. We choose this process as a reference

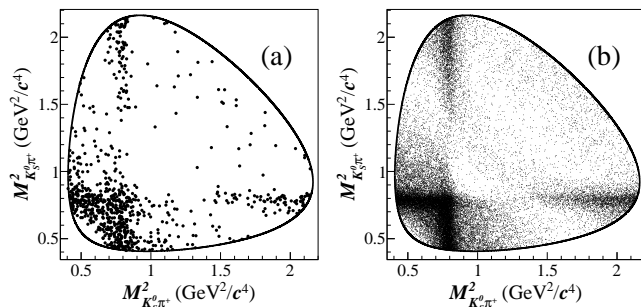


FIG. 1. Dalitz plot of $M_{K_S^0 \pi^+}^2$ versus $M_{K_S^0 K_S^0}^2$ for $D_s^+ \rightarrow K_S^0 K_S^0 \pi^+$, symmetrized for the indistinguishable K_S^0 candidates (two entries per event), of (a) the sum of all data samples and (b) the signal MC samples generated based on the amplitude analysis result. The black curve indicates the kinematic boundary.

so that the magnitudes and phases of other amplitudes are to be understood as relative values with respect to this reference amplitude. The purity is a fixed quantity in the fit. Other possible contributions from resonances such as $K_1(1410)^+$, $K_0^*(1430)^+$, $a_0(980)$, $f_0(980)$, $f_2(1270)$, $a_2(1320)$, $f_0(1370)$, $a_0(1450)$, $f_0(1500)$, $f_2(1525)$, $a_2(1700)$ and $S(1710)$ are added to the fit one at a time. The masses and widths of all resonances are fixed to the known values [6] apart from those of the $S(1710)$. The statistical significance of each new amplitude is calculated from the change of the log-likelihood taking the change in the number of degrees of freedom into account. Various combinations of these resonances are also tested. In addition to the reference amplitude $D_s^+ \rightarrow K_S^0 K^*(892)^+$, the amplitude for the decay $D_s^+ \rightarrow S(1710)\pi^+$ is found to have a significance larger than 10σ . No other contribution has a significance of more than 3σ . The significance of a $a_0(980)/f_0(980)$ contribution is less than 0.1σ . The Dalitz plot of the signal MC sample generated based on the result of the

amplitude analysis is shown in Fig. 1(b). The mass projections of the fit are shown in Fig. 2. The goodness of fit is $\chi^2/\text{NDOF} = 15.9/19 = 0.8$ for Fig. 2(a) and $28.8/32 = 0.9$ for Fig. 2(b), where NDOF is the number of degrees of freedom. In the goodness of fit calculation, we merge neighboring bins until each bin has at least 10 entries.

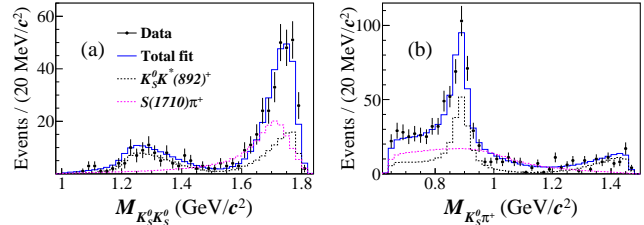


FIG. 2. Distribution of (a) $M_{K_S^0 K_S^0}^2$ and (b) $M_{K_S^0 \pi^+}^2$ from the nominal fit. The distribution of $M_{K_S^0 \pi^+}^2$ contains two entries per event, one for each K_S^0 . The data samples are represented by points with uncertainties and the fit results by the blue lines. Colored dashed lines show the individual components of the fit model. Due to interference effects, the total PDF is not necessarily equal to the sum of the components.

The contribution of the n th amplitude relative to the total BF is quantified by the fit fraction (FF) defined as $\text{FF}_n = \int |\rho_n A_n|^2 dR_3 / \int |M|^2 dR_3$. The FFs for both amplitudes and the phase difference relative to the reference process are listed in Table I. The sum of the two FFs is 89.8%. The Breit-Wigner mass and width of the $S(1710)$ are determined to be $(1.723 \pm 0.011_{\text{stat}} \pm 0.002_{\text{syst}}) \text{ GeV}/c^2$ and $(0.140 \pm 0.014_{\text{stat}} \pm 0.004_{\text{syst}}) \text{ GeV}/c^2$, respectively.

TABLE I. Fit Fractions (FF) for the two amplitudes, and phase difference to the reference process. The first and the second uncertainties are statistical and systematic, respectively. The sum of the two FFs is 89.8%.

Amplitude	Phase	FF (%)
$D_s^+ \rightarrow K_S^0 K^*(892)^+$	0.0(fixed)	$43.5 \pm 3.9 \pm 0.5$
$D_s^+ \rightarrow S(1710)\pi^+$	$2.3 \pm 0.1 \pm 0.1$	$46.3 \pm 4.0 \pm 1.2$

Systematic uncertainties for the results of the amplitude analysis, including the phase difference, FFs, and the mass and the width of the $S(1710)$, are determined by differences between the results of the nominal fit and fits with the following variations. The mass and the width of the $K^*(892)^+$ are shifted by their uncertainties [6]. The radii of the Blatt-Weisskopf barrier factors are varied from their nominal values of 5 GeV^{-1} and 3 GeV^{-1} (for the D_s^+ meson and the intermediate resonances, respectively) by $\pm 1 \text{ GeV}^{-1}$. The uncertainties associated with the size of the background sample are studied by varying the purity within its statistical uncertainty. An

alternative background sample is used to determine the background PDF, where the relative fractions of background processes from direct $q\bar{q}$ and non- $D_s^{*\pm}D_s^\mp$ open-charm processes are varied by the statistical uncertainties of the known cross sections. To estimate the systematic uncertainty related to the reconstruction efficiency, the amplitude analysis is performed varying the particle-identification and tracking efficiencies according to their uncertainties. The total uncertainties are obtained by adding these contributions in quadrature.

The BF of $D_s^+ \rightarrow K_S^0 K_S^0 \pi^+$ is measured with the DT technique using the same tag modes and event selection criteria as in the amplitude analysis. However, the kinematic fit is not applied. We require the momentum of the isolated π^+ to be greater than > 0.1 GeV/c to remove soft pions from D^{*+} decays. For each tag mode, the best ST candidate of the tag D_s^- is chosen as the combination with the recoiling mass closest to the known D_s^{*+} mass [6] and the best DT candidate is chosen as the combination with the average mass of the tag D_s^- (M_{tag}) and the signal D_s^+ (M_{sig}) closest to the D_s^{*+} mass. The BF is given by [23, 24]

$$\mathcal{B}_{\text{sig}} = \frac{N_{\text{total, sig}}^{\text{DT}}}{\sum_{\alpha, i} N_{\alpha, i}^{\text{ST}} \epsilon_{\alpha, \text{sig}, i}^{\text{DT}} / \epsilon_{\alpha, i}^{\text{ST}}}, \quad (1)$$

where α runs over the various tag modes, and i denotes the different center-of-mass energies. The ST yields in data $N_{\alpha, i}^{\text{ST}}$ and the DT yield $N_{\text{total, sig}}^{\text{DT}}$ are determined by fits to the M_{tag} and M_{sig} distributions shown in Figs. 3(a-f) and Fig. 3(i), respectively. The signal shape is modeled with the MC-simulated shape convolved with a Gaussian function. In the fits to the M_{tag} distributions, the background is parameterized as a second-order Chebyshev polynomial. For the tag modes $D_s^- \rightarrow K_S^0 K^-$ and $D_s^- \rightarrow \pi^- \eta'$, MC simulations of the decays $D^- \rightarrow K_S^0 \pi^-$ and $D_s^- \rightarrow \eta \pi^+ \pi^- \pi^-$ are added to the background to account for these peaking background contributions. In the fit to the M_{sig} distribution, the background is described by the background MC. The corresponding efficiencies ϵ are obtained by analyzing the inclusive MC samples, with the signal events for $D_s^+ \rightarrow K_S^0 K_S^0 \pi^+$ generated based on the results of the amplitude analysis. The total ST yields of all tag modes and the DT yields are 531217 ± 2235 and 371 ± 21 , respectively. The BF of $D_s^+ \rightarrow K_S^0 K_S^0 \pi^+$ is determined to be $(0.68 \pm 0.04_{\text{stat}} \pm 0.01_{\text{syst}})\%$.

We consider the following systematic uncertainties in the measurement of the BF. Varying the signal and background shapes and taking into account the background fluctuation, the uncertainty on the total number of ST D_s^- candidates is 0.4%.

The uncertainty associated with the background shape in the fit to the DT M_{sig} distribution is 0.3%, determined by replacing the nominal background shape with

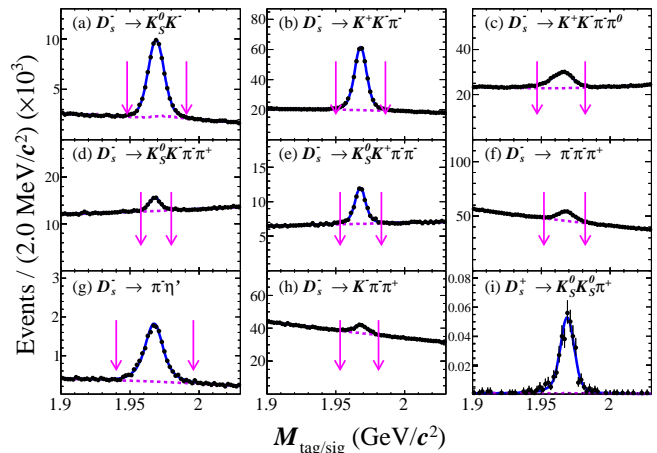


FIG. 3. Fits to (a)-(h) the M_{tag} distributions of the ST candidates and (i) the M_{sig} distribution of the DT signal candidates. The data samples are represented by points with uncertainties, the total fit results by solid blue lines and the background contributions by dashed violet lines. The pairs of pink arrows indicate the signal regions.

a second-order Chebyshev function and taking the difference between the two results. The uncertainty of the K_S^0 reconstruction efficiency is examined using control samples of $J/\psi \rightarrow K_S^0 K^\pm \pi^\mp$ and $\phi K_S^0 K^\pm \pi^\mp$ decays, and the data-MC efficiency ratio is $(101.01 \pm 0.53)\%$ [31]. We correct the signal efficiencies by this factor, and use the uncertainty of 0.53% as a systematic uncertainty. The π^+ tracking efficiencies are studied with $e^+e^- \rightarrow K^+ K^- \pi^+ \pi^-$ events. The data-MC efficiency differences of the π^+ particle-identification and tracking are both 1.0%. The uncertainty from the signal MC based on the results of the amplitude analysis is studied by varying the fit parameters according to the covariance matrix. The change of signal efficiency is estimated to be 0.5%. The uncertainty due to the limited MC sample size is obtained from $\sqrt{\sum_{\alpha, i} (f_{\alpha, i} \frac{\delta \epsilon_{\alpha, i}}{\epsilon_{\alpha, i}})^2}$, where $f_{\alpha, i}$ is the tag yield fraction, and ϵ_i and $\delta \epsilon_i$ are the signal efficiency and the corresponding uncertainty of tag mode α and center-of-mass energy i , respectively. It is found to be 0.2%. In total, the systematic uncertainty on the branching fraction is 1.9%.

In summary, we present the first amplitude analysis of the decay $D_s^+ \rightarrow K_S^0 K_S^0 \pi^+$ using 6.32 fb^{-1} of e^+e^- annihilation data taken at center-of-mass energies between 4.178 and 4.226 GeV. The results are listed in Table I. The Breit-Wigner mass and width of the $S(1710)$ are measured to be $(1.723 \pm 0.011_{\text{stat}} \pm 0.002_{\text{syst}}) \text{ GeV}/c^2$ and $(0.140 \pm 0.014_{\text{stat}} \pm 0.004_{\text{syst}}) \text{ GeV}/c^2$, respectively. These parameters are consistent with the PDG evaluation for the $f_0(1710)$ within 1.2σ and 0.7σ , respectively [6].

The BF of $D_s^+ \rightarrow K_S^0 K_S^0 \pi^+$ is determined to be

$(0.68 \pm 0.04_{\text{stat}} \pm 0.01_{\text{syst}})\%$, which is consistent with the CLEO result $\mathcal{B}(D_s^+ \rightarrow K_S^0 K_S^0 \pi^+) = (0.77 \pm 0.05_{\text{stat}} \pm 0.03_{\text{syst}})\%$ [6, 11] within 1.3σ . The BF for the two intermediate processes are calculated with $\mathcal{B}_i = \text{FF}_i \times \mathcal{B}(D_s^+ \rightarrow K_S^0 K_S^0 \pi^+)$, as shown in Table II. The BF of $D_s^+ \rightarrow K_S^0 K^*(892)^+, K^*(892)^+ \rightarrow K_S^0 \pi^+$ is determined to be $(3.0 \pm 0.3_{\text{stat}} \pm 0.1_{\text{syst}}) \times 10^{-3}$. This leads to $\mathcal{B}(D_s^+ \rightarrow \bar{K}^0 K^*(892)^+) = (1.8 \pm 0.2_{\text{stat}} \pm 0.1_{\text{syst}})\%$ which deviates from the CLEO result of this BF, $(5.4 \pm 1.2)\%$ [6, 32], by 2.9σ . However, Ref. [32] does not consider interference terms.

Because a significant $D_s^+ \rightarrow f_0(980)/a_0(980)^0 \pi^+$ contribution is observed in the amplitude analysis of $D_s^+ \rightarrow K^+ K^- \pi^+$ [3], one would expect that about 10% of the signal comes from $D_s^+ \rightarrow f_0(980)/a_0(980)^0 \pi^+$ with $f_0(980)/a_0(980)^0 \rightarrow K_S^0 K_S^0$ [6]. However, almost no signal populates the region below $1.1 \text{ GeV}/c^2$ in the $K_S^0 K_S^0$ mass spectrum. This suppression can likely be attributed to destructive interference between $a_0(980)^0$ and $f_0(980)$ in decays to two neutral kaons. The same interference term would then be constructive in decays to two charged kaons, explaining the large branching fraction observed there. On the other hand, an enhancement is seen in the $K_S^0 K_S^0$ mass spectrum around $1.7 \text{ GeV}/c^2$. Ref. [3] reports $\mathcal{B}(D_s^+ \rightarrow f_0(1710)\pi^+, f_0(1710) \rightarrow K^+ K^-) = (0.10 \pm 0.02_{\text{stat}} \pm 0.03_{\text{syst}})\%$. This corresponds to an expected BF of about 5×10^{-4} for $D_s^+ \rightarrow f_0(1710)\pi^+, f_0(1710) \rightarrow K_S^0 K_S^0$, based on isospin symmetry predicting the ratio $\frac{\mathcal{B}(f_0(1710) \rightarrow K^+ K^-)}{\mathcal{B}(f_0(1710) \rightarrow K_S^0 K_S^0)}$ to be two. In our amplitude analysis, we determine this BF to be $(3.1 \pm 0.3_{\text{stat}} \pm 0.1_{\text{syst}}) \times 10^{-3}$, which is one order of magnitude larger than the expectation. Based on the same argument concerning the difference in interference between pairs of charged and neutral kaons in isospin one and isospin zero configurations, this observation implies the existence of an isospin one partner of the $f_0(1710)$ meson, the $a_0(1710)^0$, as proposed by Ref. [1] and as recently observed in Ref. [5]. The $f_0(1710)$ and $a_0(1710)^0$ amplitudes could then interfere constructively in decays to two neutral kaons and destructively in decays to two charged kaons, explaining the different observations made in this work and in Ref. [3]. A simultaneous amplitude analysis of $D_s^+ \rightarrow K^+ K^- \pi^+$ and $D_s^+ \rightarrow K_S^0 K_S^0 \pi^+$ can further clarify this situation. In addition, a charged partner of $a_0(1710)^0$ is expected to be visible in the $K_S^0 K^+$ mass spectrum in the related decay $D_s^+ \rightarrow K_S^0 K^+ \pi^0$ [33].

The BESIII collaboration thanks the staff of BEPCII and the IHEP computing center for their strong support. This work is supported in part by National Key R&D Program of China under Contracts Nos. 2020YFA0406400, 2020YFA0406300; National Natural Science Foundation of China (NSFC) under Contracts Nos. 11625523, 11635010, 11735014, 11822506, 11835012, 11875054, 11935015, 11935016, 11935018, 11961141012, 12022510, 12025502, 12035009, 12035013,

TABLE II. BFs for amplitudes with the final state $K_S^0 K_S^0 \pi^+$. The first and the second uncertainties are statistical and systematic, respectively.

Amplitude	BF (10^{-3})
$D_s^+ \rightarrow K_S^0 K^*(892)^+ \rightarrow K_S^0 K_S^0 \pi^+$	$3.0 \pm 0.3 \pm 0.1$
$D_s^+ \rightarrow S(1710)\pi^+ \rightarrow K_S^0 K_S^0 \pi^+$	$3.1 \pm 0.3 \pm 0.1$

12061131003; the Chinese Academy of Sciences (CAS) Large-Scale Scientific Facility Program; Joint Large-Scale Scientific Facility Funds of the NSFC and CAS under Contracts Nos. U2032104, U1732263, U1832207; CAS Key Research Program of Frontier Sciences under Contract No. QYZDJ-SSW-SLH040; 100 Talents Program of CAS; INPAC and Shanghai Key Laboratory for Particle Physics and Cosmology; ERC under Contract No. 758462; European Union Horizon 2020 research and innovation programme under Contract No. Marie Skłodowska-Curie grant agreement No 894790; German Research Foundation DFG under Contracts Nos. 443159800, Collaborative Research Center CRC 1044, FOR 2359, GRK 2149; Istituto Nazionale di Fisica Nucleare, Italy; Ministry of Development of Turkey under Contract No. DPT2006K-120470; National Science and Technology fund; Olle Engkvist Foundation under Contract No. 200-0605; STFC (United Kingdom); The Knut and Alice Wallenberg Foundation (Sweden) under Contract No. 2016.0157; The Royal Society, UK under Contracts Nos. DH140054, DH160214; The Swedish Research Council; U. S. Department of Energy under Contracts Nos. DE-FG02-05ER41374, DE-SC-0012069.

-
- [1] E. Klempt, *Phys. Lett. B* **820**, 136512 (2021).
 - [2] A. V. Sarantsev, I. Denisenko, U. Thoma, and E. Klempt, *Phys. Lett. B* **816**, 136227 (2021).
 - [3] M. Ablikim *et al.* (BESIII Collaboration), *Phys. Rev. D* **104**, 012016 (2021).
 - [4] P. del Amo Sanchez *et al.* (BaBar Collaboration), *Phys. Rev. D* **83**, 052001 (2011).
 - [5] J. P. Lees *et al.* (BaBar Collaboration), [arXiv:2106.05157 \[hep-ex\]](https://arxiv.org/abs/2106.05157).
 - [6] P. A. Zyla *et al.* (Particle Data Group), *Prog. Theor. Exp. Phys.* **2020**, 083C01 (2020) and 2021 update.
 - [7] B. Bhattacharya and J. L. Rosner, *Phys. Rev. D* **79**, 034016 (2009).
 - [8] H. Y. Cheng and C. W. Chiang, *Phys. Rev. D* **81**, 074021 (2010).
 - [9] F. S. Yu, X. X. Wang, and C. D. Lü, *Phys. Rev. D* **84**, 074019 (2011).
 - [10] Y. K. Hsiao, Y. Yu, and B. C. Ke, *Eur. Phys. J. C* **80**, 895 (2020).
 - [11] P. U. E. Onyisi *et al.* (CLEO Collaboration), *Phys. Rev. D* **88**, 032009 (2013).
 - [12] M. Ablikim *et al.* (BESIII Collaboration),

- Nucl. Instrum. Methods Phys. Res. Sect. A **614**, 345 (2010).
- [13] M. Ablikim *et al.* (BESIII Collaboration), *Chin. Phys. C* **44**, 040001 (2020).
- [14] C. H. Yu *et al.*, Proceedings of IPAC2016, Busan, Korea, 2016, doi:10.18429/JACoW-IPAC2016-TUYA01.
- [15] X. Li *et al.*, *Radiat. Detect. Technol. Methods* **1**, 13 (2017); Y. X. Guo *et al.*, *Radiat. Detect. Technol. Methods* **1**, 15 (2017).
- [16] S. Agostinelli *et al.* (GEANT4 Collaboration), *Nucl. Instrum. Meth. A* **506**, 250 (2003).
- [17] S. Jadach, B. F. L. Ward, and Z. Was, *Phys. Rev. D* **63**, 113009 (2001); *Comput. Phys. Commun.* **130**, 260 (2000).
- [18] D. J. Lange, *Nucl. Instrum. Meth. A* **462**, 152 (2001); R. G. Ping, *Chin. Phys. C* **32**, 599 (2008).
- [19] J. C. Chen, G. S. Huang, X. R. Qi, D. H. Zhang, and Y. S. Zhu, *Phys. Rev. D* **62**, 034003 (2000); R. L. Yang, R. G. Ping and H. Chen, *Chin. Phys. Lett.* **31**, 061301 (2014).
- [20] E. Richter-Was, *Phys. Lett. B* **303**, 163 (1993).
- [21] J. Adler *et al.* (MARK-III Collaboration), *Phys. Rev. Lett.* **62**, 1821 (1989).
- [22] M. Ablikim *et al.* (BESIII Collaboration), *Phys. Rev. D* **103**, 092004 (2021).
- [23] M. Ablikim *et al.* (BESIII Collaboration), *J. High Energy. Phys.* **2021**, 181 (2021).
- [24] M. Ablikim *et al.* (BESIII Collaboration), *Phys. Rev. D* **103**, 092006 (2021).
- [25] B. S. Zou and D. V. Bugg, *Eur. Phys. J. A* **16**, 537 (2003).
- [26] J. M. Blatt and V. F. Weisskopf, *Theoretical Nuclear Physics* (John Wiley & Sons, New York, 1973).
- [27] J. D. Jackson, *N. Cimento* **34**, 1644 (1964).
- [28] M. Artuso *et al.* (CLEO Collaboration), *Phys. Rev. D* **85**, 122002 (2012).
- [29] W. Verkerke and D. P. Kirkby, *RooFit Users Manual v2.07* (2006).
- [30] K. Cranmer, *Comput. Phys. Commun.* **136**, 198 (2001).
- [31] M. Ablikim *et al.* (BESIII Collaboration), *Phys. Rev. D* **92**, 112008 (2015).
- [32] W. Y. Chen *et al.* (CLEO Collaboration), *Phys. Lett. B* **226**, 192 (1989).
- [33] BESIII Collaboration, “Study of $D_s^+ \rightarrow K_S^0 K^+ \pi^0$,” to be submitted.